

Microwave-Assisted Hydrothermal Synthesis and Optical Characterization of SnO₂ Nanoparticles

P. Boroojerdian

Department of Passive Defense, Malek Ashtar University of Technology, Tehran, I. R. Iran.

(*) Corresponding author: boroojerdian89@gmail.com

(Received: 28 June 2013 and Accepted: 27 Sep. 2013)

Abstract:

Semiconductor nanoparticles exhibit size dependent properties due to quantum confinement effect that are not present in their bulk counterparts. In this work, extremely fine and pure SnO₂ nanoparticles of ~1.1 nm size were synthesized by a solution process, in which amorphous precipitate of SnO₂ was crystallized by microwave heating. The particles sizes varied from ~1.1 to ~2.7 nm. By XRD analysis, the particle size, crystal structure and purity of the samples were determined. The UV-Vis measurements of SnO₂ nanoparticles, showed that, excitonic peaks existed at ~237, ~250 and ~279 nm corresponding to ~1.1, ~2 and ~2.7 nm clusters respectively. The STM analysis showed that the nanoparticles were spherical in shape, having narrow size distribution.

Keywords: Tin Oxide, Nanoparticles, Microwave heating, Semiconductors, SnO₂

1. INTRODUCTION

Over the past few decades, nanoparticles and nanostructural materials have become an attractive group of materials due to their novel properties [1-3]. In the nanometer region, various quantum mechanical effects, such as the increase in the energy gap of a semiconducting material with a reduction in size are observed [4,5].

The possibility of a continuous tuning of electronic and optical properties of materials by particle size variation is viewed as a promising trend for future applications [6]. The nanoparticles of semiconducting materials, including SnO₂ have been the subject of numerous investigations in the past decades.

If a semiconductor particle becomes smaller than Bohr radius of the exciton, the so called quantum size effect occurs [7]. As a result, the gap of semiconducting material increases, and at the edges of the (valence and conduction) bands, discrete energy levels occur. Therefore, a blue shift is readily

observable in the absorption edge. Shift in the excitonic peak position occurring due to reduction of size is given as follows according to the effective mass approximation theory [8],

$$\Delta E = \frac{h\pi^2}{2R^2} \left[\frac{1}{m_e} + \frac{1}{m_h} \right] - \frac{1.8e^2}{\epsilon R} + \text{small terms}$$

where R is the cluster radius. Interestingly, the oscillator strength of the exciton also begins to increase with the reduction of the particle size [7].

SnO₂, a wide band gap n-type semiconductor (with a E_g = 3.6-3.8 eV [9-10]), has a wide range of applications such as in gas sensors [11-12], transparent conducting electrodes [13], dye-sensitized solar cells [14-15], catalysts [16], white pigments for conducting coatings [17] and secondary Lithium batteries [18].

Therefore, the synthesis of high quality SnO₂ nanoparticles with a diameter less than or comparable to excitonic Bohr radius (~ 2.7 nm) is extremely important from the basic research and application point of view [25].

A variety of techniques such as sonochemical [19], hydrothermal [20], solvothermal [21], sol-gel [22], microwave-assisted hydrothermal [23] and spray pyrolysis [24] have been proposed to synthesize SnO₂ nanoparticles. Among the chemical methods, microwave-assisted hydrothermal synthesis has the advantage of having short processing time, good control of particle size, uniform nucleation and purity of the final product.

In the past, many attempts have been made to prepare SnO₂ ultrafine nanoparticles using various methods. For example, Zhang et al. [25], Zhu et al. [26] and Pinna et al. [27] have reported the synthesis of SnO₂ nanoparticles ranging from 2 to 5 nm size, but there is no clear evidence of the quantum size effect (excitonic peaks) in their UV-Vis Spectra.

Here, in this work we report the single phase pure SnO₂ nanoparticles synthesized by microwave heating of the reacting solution. The solutions with constant molarities were irradiated with microwaves for various durations to obtain different sizes of nanoparticles. For the first time, we carried out a systematic particle size variation from ~1.1 nm to ~2.7 nm. The excitonic peaks observed in the optical absorption spectra, also exhibited a blue shift due to the reduction in the particle size. Bulk SnO₂ had an energy gap of ~3.7 eV which rose up to 5.22 eV due to quantum confinement at ~1.1 nm cluster size.

2. EXPERIMENTAL

The following method was used for synthesizing the SnO₂ nanoparticles. A first 100 ml aqueous solution (10⁻² M and pH=1.3) was prepared by dissolving appropriate amount of SnCl₄·5H₂O in dilute HCl. A second aqueous solution (10⁻² M) was prepared by mixing appropriate amount of NH₄OH in de-ionized water.

The latter solution was then added drop by drop to the former solution at room temperature by moderate stirring to obtain a precipitate until the pH of the solution increased to 4. After the reaction completed, the precipitate was washed several times with de-ionized water and ethanol to remove excess ions. The precipitate was dispersed in water and then irradiated with microwave (Samsung, Cambi model 2450 MHz). Several experiments were carried out in order to investigate the effect of irradiation time at

constant 900 watt irradiation power. The parameters studied are shown in table 1.

The samples were characterized by X-Ray Diffraction (XRD), using a Philips PW 1830 diffractometer (CuKα = 1.5418 Å, 40 KV, 30 mA) and the optical absorbance spectra of the samples were recorded by a Hitachi UV-Vis 3310 spectrophotometer. The shape and size of nanoparticles was observed by Scanning Tunneling Microscopy (STM) with Natsyco model SS/1.

3. RESULTS AND DISCUSSION

X-Ray diffraction technique was used to identify the crystalline structure (phase) as well as the mean particle size of the samples. Figure 1 illustrates the XRD patterns of the SnO₂ samples prepared under various durations of microwave irradiation (5, 10 and 15 minutes) and molarity (1 × 10⁻² M) at constant 900 watt irradiation power.

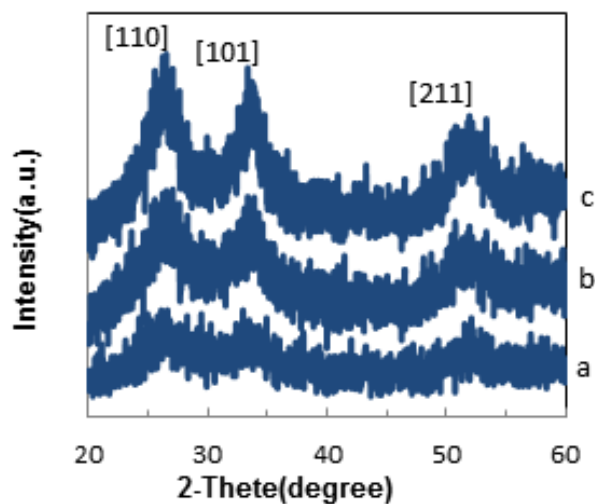


Figure 1: XRD patterns of SnO₂ nanoparticles treated at 900 watt irradiation power for: a) 5 minutes b) 10 minutes and c) 15 minutes.

All patterns exhibit three broad peaks which are attributed to the tetragonal phase of SnO₂. However, samples treated under longer durations of irradiation show more intense peaks compared to the samples treated for shorter durations. This is the indication of particle size growth. The agreement of the d-values of observed peaks and those reported for SnO₂ is excellent [28].

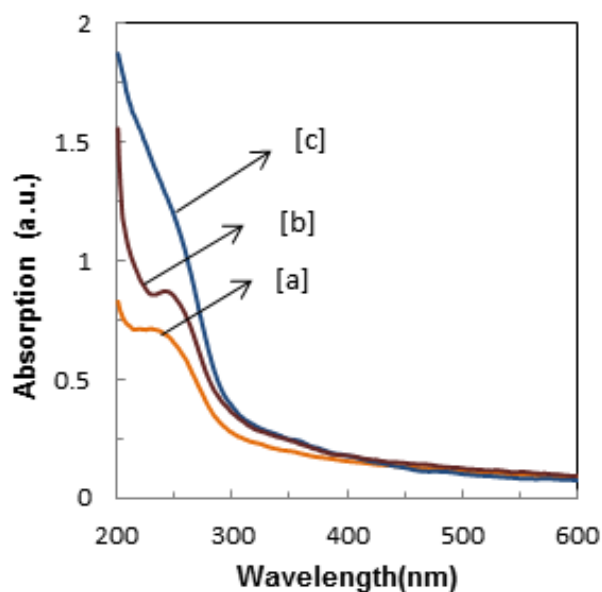


Figure 2: Optical absorption of SnO₂ nanoparticles prepared at different durations of, a) 5 minutes b) 10 minutes and c) 15 minutes at 900 watt microwave irradiation power

The XRD results also have a resemblance to the diffraction patterns shown in references [20] and [22]. Thus, here we observe a variation in the particle size due to variation of irradiation time. The average particle size were determined from full-width at half-maximum (FWHM) of the most intense peaks (110) at $2\theta=26.588$ using scherrer's equation, i.e., $D = 0.9\lambda/B\cos\theta$, where D is the average grain size, λ is the X-ray wavelength, B is the FWHM of (110) the peak. The calculated average sizes of the particles

obtained (from Figure 1) were ~ 1.5 , ~ 2.3 and ~ 3 nm respectively. The broad diffraction peaks reveal the very small size of the SnO₂ nanoparticles.

It is believed that the band gap of semiconductor nanoparticles increases with the decrease of its particle size, and the absorption edge will be blue shifted due to quantum size effect. Figure 2 shows the optical absorption of the SnO₂ samples with the variation of sizes (from Figure 1) ranging from ~ 1.5 ~ 3 nm. The reported band gap value of bulk is ~ 3.6 - 3.8 eV at the expected absorption peak of ~ 335 - 344 nm [8-9].

The excitonic peaks are evident in the samples irradiated at 900 watt microwave power from 5 to 15 minutes with molarity remaining constant at 10^{-2} M. For the finest particle (sample SnO₂-1), the excitonic peak appeared at ~ 237 nm (~ 5.22 eV). For samples irradiated for 10 and 15 minutes, the peaks shifted to ~ 250 and ~ 279 nm respectively.

For the sample irradiated for more than 15 minutes, no excitonic peak was observed. This is the indication of particle size growth (beyond Bohr radius). Here, it can be seen that, the excitonic peaks for different samples have shifted from ~ 237 nm to ~ 279 nm corresponding to energy gaps from ~ 5.22 eV to ~ 4.44 eV. In Table 1, position of excitonic peaks (energy gap) and the particle size (calculated from XRD patterns) are shown at various durations of microwave irradiation. In order to confirm the particle size and shape of the particles, STM was performed for the SnO₂ sample obtained by irradiation of the precipitate (1×10^{-2} molarity) at 900 watt for 5 minutes.

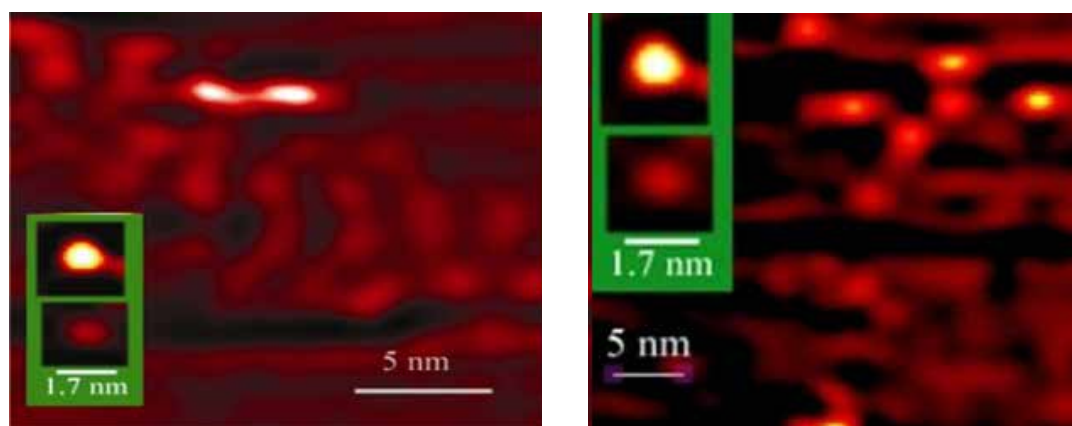


Figure 3: STM images of the SnO₂

Table 1: Concentration, conditions, particle sizes and positions of excitonic peaks of hydrothermal treatment applied to the starting solutions.

Sample	SnCl ₄ .5H ₂ O molarity (mol/L)	Molarity of NH ₄ OH(mol/L)	Microwave power (W)	Irradiation Time (minute)	Excitonic Peak Position(nm)	Calculated Particle Size(nm)	Energy Gap(eV)
SnO ₂ -1	10 ⁻²	1×10 ⁻²	900	5	237	1.5	5.22
SnO ₂ -2	10 ⁻²	1×10 ⁻²	900	10	250	2.3	4.96
SnO ₂ -3	10 ⁻²	1×10 ⁻²	900	15	279	3	4.44

From Figure 3, it is observed that the particles are spherical and highly monodispersed. It can be noticed that the particle size is ~1.1 nm. The size is slightly smaller but still closely matches with that estimated from the scherrer formula (1.5 nm).

4. CONCLUSION

By using microwave irradiation, SnO₂ nanoparticles with narrow size distribution of various sizes (comparable or less than Bohr radius) were obtained. The SnO₂ samples showed strong excitonic peaks in the UV-Vis absorption spectra which were absent in SnO₂ bulk sample. A blue shift of up to ~237 nm corresponding to an energy gap of ~5.22 eV was observed for the finest particle size of ~1.1 nm. From the STM images, the narrow size distribution of the particles was also determined. Hence, the blue shift in the UV-Vis absorption spectra, the line broadening in the XRD pattern and the size in the STM image, all confirmed that the nanoparticles synthesized here were indeed in the quantum confinement region.

REFERENCES

1. R. Rossetti, S. Nakahara, L. E. Brus, J. Chem. Phys.: Vol. 79, (1983), pp. 1086-1088.
2. Y. Nosaka, K. Yamaguchi, H. Miyama and M. Hayashi, Chem. Lett.: Vol. 17,4, (1988), pp. 605-608.
3. N. Herron, Y. Wang, H. Eckert: J. Am. Chem. Soc., Vol. 112, (1990), pp. 1322-1326.
4. M. Kundu, A. A. Khosravi, P. Singh, S. K. Kulkarni: J. Mater. Sci., Vol. 23, (1997), pp. 245-258.
5. G. Nabyouni, P. Boroojerdian, K. Hedayati, D. Ghanbari: High Temp. Mater. Proc., Vol. 31, (2012), pp. 723-727.
6. S. Hingorani, V. Pillai, P. Kumar, M. S. Multani, D. O. Shah: Mater. Res. Bull., Vol. 28, (1993), pp. 69-73.
7. M. H. Majlesara, P. Boroojerdian, Z. Javadi, S. Zahedi, M. Morshedian: Micro & Nano Letters, Vol. 6, (2011), pp. 249-252.
8. L. E. Brus: J. Phys. Chem., 90, (1986), 2555-2560.
9. V. T. Agekyan: Phys. Status solidi, A Vol. 43, (1971), pp. 11-33.
10. J. Rockenberger, U. Felde, M. Tischer, L. Troger, M. Haase, H. Weller: J. Chem. Phys., Vol. 112, (2000), pp. 4296-4304.
11. J. X. Zhou, M. S. Zhang, J. M. Hong, J. L. Fang, J. L. Fang, Z. Yin: Appl. Phys., A Vol. 81, (2005), pp. 177-182.
12. A. Cabot, A. Vila, J. R. Moronte: Sens. Actuators, B Vol. 84, (2002), pp. 12-20.
13. Y. S. He, J. C. Cambell, R. C. Murphy, M. F. Arendt, J. S. Swinnea: J. Mater. Res., Vol. 8, (1993), pp. 3131-3134.
14. S. Chappel, A. Zaban: Solar Energy Mater. Solar Cells, Vol. 77, (2002), pp. 141-146.
15. A. Kay, M. Gratzel: Chem. Mater., Vol. 14, (2002), pp. 2930-2935.
16. P. W. Park, H. H. Kung, D. W. Kim, M. C. Kung: J.

- Catal., Vol. 184, (1999), pp. 440-445.
17. P. Olivi, E. C. P. Souza, E. Longo, J. A. Varela, L.O.S. Bulhoes: J. Electrochem. Soc., Vol. 140, (1993), pp. 81-82.
 18. A. C. Bose, D. Kalpana, P. Thangadurai, S. Ramasamy: J. Power sources, Vol. 107, (2002), pp. 138-141.
 19. L. H. Xian, Y. J. Zbu, S. W. Wang: Materials Chemistry and physics, Vol. 88, (2004), pp. 421-426.
 20. Z. Li, W. Shen, X. Zhang, L. Fong, X. Zu: Colloids and surfaces A: Physicochem. Eng. Aspects, Vol. 327, (2008), pp. 17-20.
 21. Z. Han, N. F. Li, W. Zhang, H. Zaho, Y. Qian: Materials letters, Vol. 48, (2001), pp. 99-103.
 22. J. Zhang, L. Gao: Journal of solid state chemistry, Vol. 177, (2004), pp. 1425-1430.
 23. T. Krishnakumar, N. Pinna, K.P Kumari, K. Perumal, R. Jayaprakash: Materials letters, Vol. 62, (2008), pp. 3437-3440.
 24. D. Briand, M. Labeau, J. F. Curie, G. Delabouglise: Sensors and Actuators B, Vol. 48, (1988), pp. 395-402.
 25. H. Zhang, N. Du, B. Chen, T. Cui, D. Yang: Materials Research Bulletin, Vol. 43, (2008), pp. 3164-3170.
 26. J. J. Zhu, Z. H. Lu, S. T. Aruna, D. Aurbach, A. Gedanken: Chem. Mater., Vol. 12, (2000), pp. 2557-2566.
 27. N. Pinna, G. Neri, M. Antonietti, M. Niederberger: Angew. Chem. Int. Ed., Vol. 43, (2004), pp. 4345-4349.
 28. Joint Committee on Powder Diffraction Standards, International Centre for Diffraction Data, Pennsylvania (1991).

